THE ASTROPHYSICAL JOURNAL, 289:765–773, 1985 February 15

THE R AQUARII SYSTEM AT OPTICAL AND RADIO WAVELENGTHS

J. M. HOLLIS
Laboratory for Astronomy and Solar Physics, NASA/GSFC

M. KAFATOS
Department of Physics, George Mason University

A. G. MICHALITSIANOS
Laboratory for Astronomy and Solar Physics, NASA/GSFC

AND

H. A. MCALISTER
Department of Physics and Astronomy, Georgia State University

Received 1984 May 21; accepted 1984 August 30

ABSTRACT

Observations of the symbiotic binary R Aquarii environment were obtained with the Very Large Array (VLA) at 2, 6, and 20 cm at the same epoch. The observed spectral index and strong linear polarization reveal that emission from the compact double radio source discovered in previous observations is nonthermal; thus, this source is not associated with R Aquarii but is an extragalactic background object. The spectral index of the compact nebula surrounding R Aquarii indicates that the emission is thermal and the nebula is ionized by an unseen, hot companion to the Mira-like variable R Aquarii. As expected, this region shows no indication of linear polarization, and we have determined a steady state mass loss of $\sim 2.7 \times 10^{-7}$ $M_\odot$ yr^{-1} from the system. However, the spectral index and polarization observations of the extended jet $\sim 6''$ away from R Aquarii indicate that this amorphous source is definitely thermal and optically thin in nature. These new observations place severe constraints on possible models which have been proposed from previous investigations. We suggest that our new observations of the jet can be best explained by enhanced mass exchange occurring periodically in the symbiotic system. Comparison of 6 cm data taken with the same VLA configuration but separated by 495 days does not indicate any appreciable morphological change or statistically significant integrated flux difference and thus suggests that on these time scales the jet is now quite stable. High-resolution white light images of R Aquarii and environs obtained with the 4 m telescope at Kitt Peak just prior to the VLA observations show a high degree of correlation with the 6 cm radio data and place a limit on the apparent visual magnitude of the compact double radio source; optical speckle interferometry failed to resolve any components in the R Aquarii system.

Subject headings: interferometry — polarization — stars: individual — stars: long-period variables — stars: radio radiation

I. INTRODUCTION

R Aquarii is a symbiotic system which contains a ~ 387 day pulsational period Mira and a hot $T_{\rm eff} \approx 2$–5×10^4 K subdwarf companion; hereafter, we will refer to these two stars as the long-period variable (LPV) and the hot companion, respectively. There are several radio features in the immediate vicinity of the R Aquarii system and these are shown best at 6 cm in Figure 1 (*middle panel*): The strongest 6 cm feature in Figure 1 is unlabeled and is a compact, unresolved H II region. Feature B in Figure 1 is a less compact, resolved H II region $\sim 6''$ northeast of the hot companion, and previous investigators (e.g., Herbig 1980) have commonly referred to B as the R Aquarii "jet." This jet is also seen in the optical photograph in Figure 2. Feature A in Figure 1 is unresolved, probably also an H II region, has been detected in the optical (cf. Sol 1983), and there is a suggestion of its presence in the Figure 2 photograph. Extremely weak feature A′ in Figure 1 may be a symmetrical counterpart to stronger feature A. All of the above radio features are embedded in nebulosity which extends $\sim 120''$ roughly centered on R Aquarii; this nebulosity has the appearance of two intersecting arcs which are prominent at optical wavelengths (cf. Sopka *et al.* 1982) but have not been detected at radio wavelengths. Moreover, recently we reported a compact double radio source (CDRS) $\sim 196''$ northeast of the LPV and suggested that the CDRS may be associated with the R Aquarii system since its peak intensity lies on the position angle defined by the jet and the LPV (Kafatos, Hollis, and Michalitsianos 1983).

This paper reports new continuum observations of all radio components of the R Aquarii system at 2, 6, and 20 cm which allow determination of polarization properties, integrated flux levels, spectral indices, and, hence, the emission mechanisms of the individual components. Moreover, complementary wide-band optical observations (predominantly at Hα and Hβ) are also reported to help determine the nature and structure of the CDRS and the R Aquarii radio jet. The results of these observations are discussed in detail with regard to models currently or previously proposed for the R Aquarii system.

II. OBSERVATIONS

a) Radio

The observations, centered on R Aquarii and the CDRS, were made 1984 February 3 with the NRAO[1] VLA in the B antenna configuration. Twenty-four antennas were employed

[1] The National Radio Astronomy Observatory is operated by Associated Universities, Inc., under contract with the National Science Foundation.

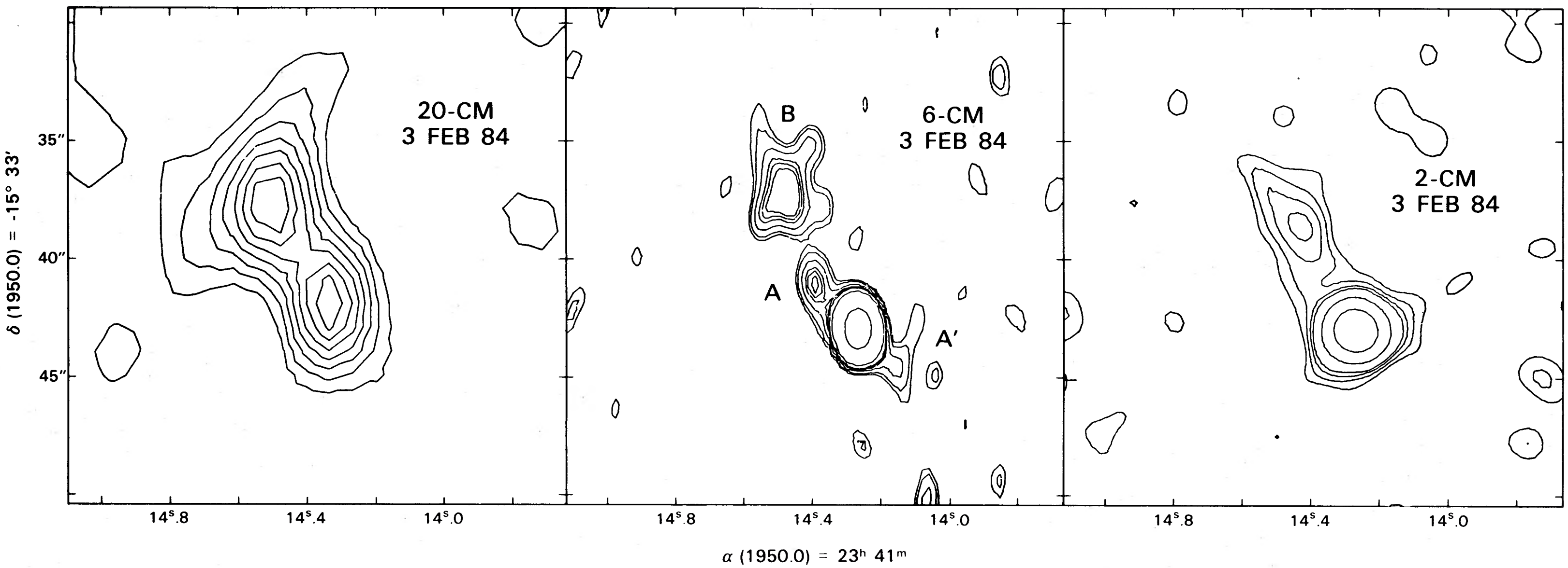

FIG. 1.—(*left*) This 20 cm map shows the jet rivals the compact H II region with regard to both peak and integrated flux (see Table 1) at this wavelength. Contour levels are 0.5, 0.8, 1.1, 1.4, 1.7, 2.0, and 2.3 mJy; peak fluxes for both blended features are each ~ 2.7 mJy per beam. The 1.4 contour level shows the approximate beam shape. (*middle*) This 6 cm map shows all the radio features so far detected in the immediate vicinity of R Aquarii. Contour levels are 0.15, 0.20, 0.30, 0.40, 0.45, 0.50, 0.75, and 3.70 mJy; peak flux for the compact H II region in this map is ~ 7.3 mJy per beam. The 3.7 contour level shows the approximate beam shape. (*right*) This 2 cm map clearly shows the jet at this wavelength for the first time. Contour levels are 0.35, 0.60, 0.85, 1.10, 2.50, and 6.20 mJy; peak flux for the compact H II region is ~ 12.4 mJy per beam. The 6.2 contour level shows the approximate beam shape.

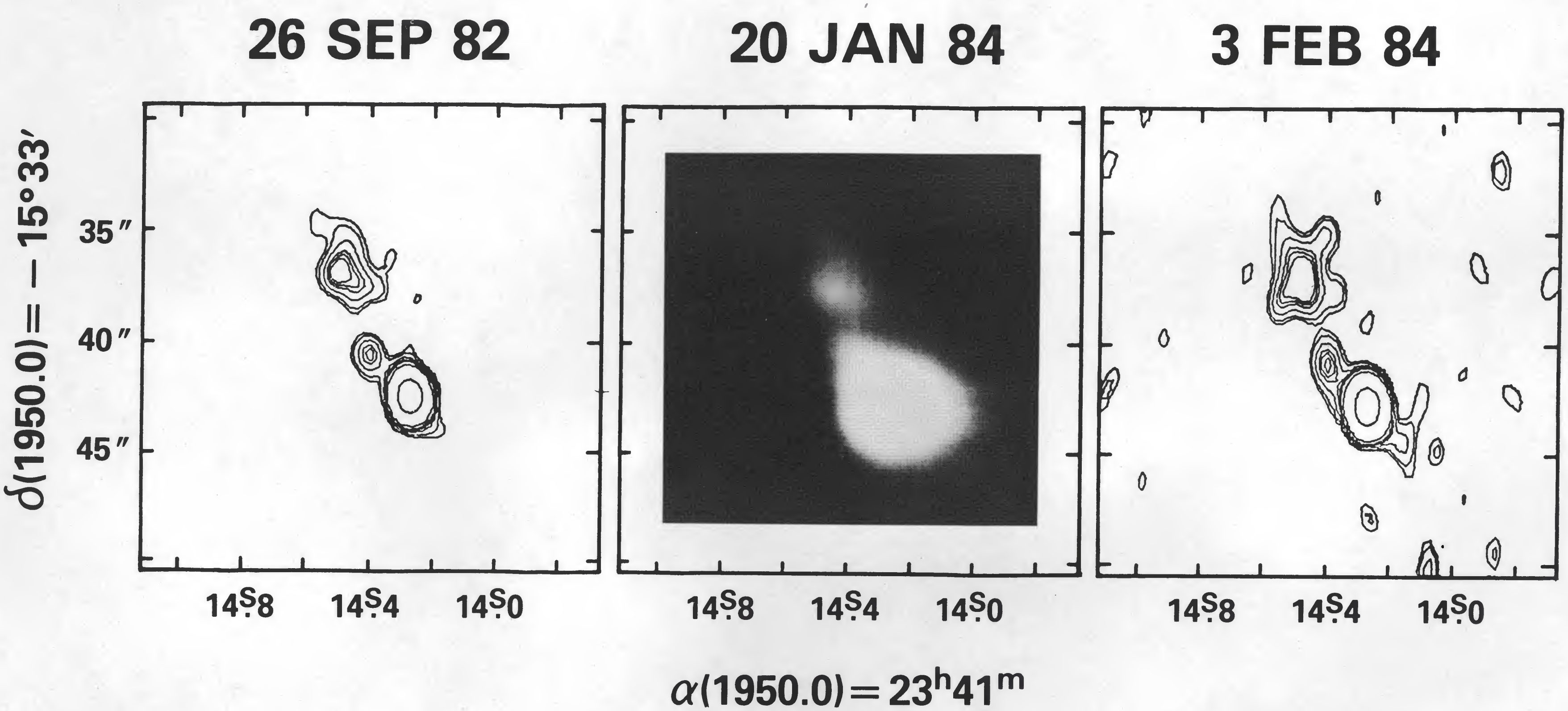

FIG. 2.—(*left*) This 6 cm has the same contour levels as the middle panel of Fig. 1 except these data have a peak flux of ~7.5 mJy per beam. We used a subset of these data to mimic the parallactic angle coverage of the data shown in the right panel of this figure; this resulted in a greater morphological similarity between the 1984 and 1982 radio data sets. However, the full data set shown here more accurately depicts the true structure as shown in the optical data of the middle panel. (*middle*) This optical photograph of R Aquarii is predominantly in the light of Hβ at 4860 Å and Hα at 6563 Å; the LPV is overexposed and the instrument suffers saturation on the LPV only. The similarity between the radio and optical data is remarkable as shown here; thus, this series of data indicate that the jet is now stable over time scales of a few years and argues for the jet's thermal nature at both optical and radio wavelengths. (*right*) This 6 cm map is a reproduction of Fig. 1 (*middle panel*) for ease of comparison with other data shown here. The apparent difference in the shape of the jet in this panel as compared to the leftmost panel is due to less complete parallactic angle coverage in the 1984 data set. However, these data more easily produce the weak feature (feature A′ in Fig. 1) seen toward the southwest of the compact H II region than that seen in the 1982 data set; thus, we may be seeing a new feature evolving; it is interesting that this new feature is symmetrically placed with regard to the stronger feature toward the immediate northeast (feature A in Fig. 1).

TABLE 1

INTEGRATED FLUXES (S_λ)[a] AND SPECTRAL INDICES (α)[a]

Feature (1)	20 cm Map (1984 Feb 3) (2)	6 cm Map (1984 Feb 3) (3)	2 cm Map (1984 Feb 3) (4)	α (1984 Feb 3) (5)	6 cm Map (1982 Sep 26) (6)
S_λ CDRS total map[b] (mJy)	17.7 ± 2.5	3.2 ± 0.7	0.9 ± 0.4	−1.30 ± 0.08	...
S_λ R Aqr Total Map[b] (mJy)	7.86 ± 1.02	12.50 ± 0.52	17.85 ± 1.00	+0.36 ± 0.02	12.03 ± 0.37
S_λ compact H II region (mJy)	3.46 ± 0.67	8.73 ± 0.34	13.94 ± 0.71	+0.61 ± 0.10	8.53 ± 0.24
S_λ feature A[c] (mJy)	...	0.90 ± 0.19	... }	−0.05 ± 0.05	{0.95 ± 0.14
S_λ feature B: jet (mJy)	4.40 ± 0.77	2.87 ± 0.34	3.91 ± 0.71}		{2.55 ± 0.24
R Aqr map type	No taper	selfcal	80 kλ taper	...	selfcal
Map noise (1 σ) (mJy per beam)	0.25	0.07	0.21	...	0.05
Convolution beam (arcsec)^2	4.87 × 2.78	1.71 × 1.03	1.77 × 1.77	...	1.42 × 1.04
Beam position angle (deg)	−2.28	−4.20	−45.11	...	−1.61

[a] Spectral indices obtained from $S_\lambda \propto \nu^\alpha$ and all quoted errors are 1 σ: The α error is the formal error on the regression line fit. The S_λ error for a given map feature is the product of the 1 σ map noise for that map times the square root of the number of beam areas encompassing the feature.

[b] 1950.0 map center coordinates for the CDRS were taken to be $\alpha = 23^h41^m20^s.495$ and $\delta = -15°30'52''.88$ and for R Aquarii were taken to be $\alpha = 23^h41^m14^s.269$ and $\delta = -15°33'42''.89$; coordinates for individual features in both maps are tabulated in Table 1 of Kafatos, Hollis, and Michalitsianos 1983.

[c] Feature A is not apparent in the 20 cm map due to the large telescope beam and in the 2 cm map due to heavy taper. However, feature A probably contaminates other features in these two maps.

at 2 cm (14,940 MHz), 6 cm (4860 MHz), and 20 cm (1490 MHz). Each observational wavelength utilized an intermediate frequency (IF) bandwidth of 50 MHz and two IF pairs, a system improvement which affords $2^{1/2}$ enhancement in signal-to-noise ratio for a given observation; doubling the number of IF pairs has occurred since our previous R Aquarii observations in 1982 September. Spacing between antenna pairs varied between 0.2 and 11.1 km which yielded synthesized CLEAN beams whose characteristics are shown in Table 1 with regard to the R Aquarii maps presented herein. Observations of each source at a particular frequency were interleaved with similar observations of 2345−167 which was used as a nearby calibrator; time dedicated to each source (i.e., R Aquarii or CDRS) was 12.5 minutes and 2.5 minutes for the calibrator, inclusive of array move time. This procedure itself was interleaved among the three observational wavelengths for a period of 8.5 hours centered on 23^h15^m LST in order to fill out the u, v plane and reduce the sidelobe levels in each synthesized map. Observations of 3C 48 were made to establish proper flux density ratios with 2345−167 and each source by assuming that 3C 48 has a constant flux density of 1.75, 5.36, and 13.76 Jy at 2, 6, and 20 cm, respectively. Moreover, 3C 138 was observed at 2, 6, and 20 cm to afford polarization calibration. Table 2 summarizes pertinent calibrator information. The calibrated amplitudes and phases for the R Aquarii–centered observations were transformed to produce the CLEANed 2, 6, and 20 cm maps shown in Figures 1 and 2 with characteristics as tabulated in Table 1.

b) *Optical*

The observations were made 1984 January 20 with the NOAO[2] 4 m telescope at Kitt Peak with two instruments: (1) the RCA 4849 intensified silicon intensified target (ISIT) camera whose spectral response is 100% at ~4800 Å, 75% at 5800 Å, 50% at 6560 Å, and 40% at 7100 Å; and (2) the ICCD speckle interferometry camera as described by McAlister, Robinson, and Marcus (1982). With the ISIT our objectives were to (*a*) obtain a high-resolution optical image of the immediate vicinity of R Aquarii in order to compare with the morphology of our VLA maps since this optical instrument is quite

[2] The National Optical Astronomy Observatories are operated by Association of Universities for Research in Astronomy, Inc., under contract with the National Science Foundation.

TABLE 2

CALIBRATION DATA

Source (1)	α(1950) (2)	δ(1950) (3)	IF Pairs (4)	20 cm Flux (Jy) (5)	6 cm Flux (Jy) (6)	2 cm Flux (Jy) (7)	UT Date (8)
3C 48	$01^h34^m49^s.832$	+32°54′20″.52	...	13.76[a]	5.36[a]	1.75[a]	...
2345−167	23 45 27.687	−16 47 52.59	AC	3.033(31)	3.037(19)	1.920(97)	1984 Feb 3
			BD	3.139(27)	3.016(19)	1.947(99)	1984 Feb 3
			AC	...	3.095(20)[b]	...	1982 Sep 26
			AC	...	3.018(13)[b]	...	1982 Sep 27
3C 138	05 18 16.532	+16 35 26.92	AC	7.532(47)	3.844(30)	1.410(48)	1984 Feb 3
			BD	7.685(46)	3.845(23)	1.428(47)	1984 Feb 3
			AC	...	4.198(33)[b]	...	1982 Sep 26
			AC	...	4.055(29)[b]	...	1982 Sep 27

[a] Assumed known (Baars *et al.* 1977); flux density errors in these columns reflect the 1 σ uncertainty in determining flux calibration ratios from observations relative to 3C 48 (see text).

[b] Table 1 of Kafatos, Hollis, and Michalitsianos 1983 have 6 cm flux values for 2345−167 and 3C 138 transposed; we note and correct the error in this tabulation.

sensitive to Hβ at 4860 Å and Hα at 6563 Å, (*b*) attempt to detect the CDRS in the optical to help decide its local or extragalactic nature, and (*c*) probe for any low surface brightness emission along the line joining the CDRS and R Aquarii. With the speckle camera our objective was to probe the immediate vicinities of R Aquarii and the CDRS for any significant high spatial resolution optical structure.

We were successful in obtaining an ISIT image of the jet near R Aquarii as is shown in Figure 2. These data represent an 8 minute integration of video frames with 0\".24 pixelation and clearly show the jet and suggest that an optical counterpart to the weak ratio feature A near R Aquarii is seen near the overexposed image of the star. The correspondence between the optical and 6 cm radio jet morphologies is highly apparent, and its significance will be discussed later. No optical counterpart of the CDRS was seen with either the ISIT or the speckle camera in the aquisition mode to a limiting magnitude of $V \approx +20$; neither were any nonstellar images detected in the ISIT along the position angle between the CDRS and R Aquarii. Moreover, no structure was observed with the speckle camera with regard to R Aquarii and its nearby hot companion even though the LPV was near minimum light.

III. RADIO AND OPTICAL MAP COMPARISONS

In order to verify the reality of the weaker radio features (e.g., features A and A′ shown in Fig. 1), we used the map self-calibration technique (i.e., routine ASCAL on the NRAO image processing system) independently on both 6 cm data sets from 1982 and 1984. As can be seen in Figure 2, both data sets processed this way qualitatively show the same features. Quantitatively, these maps were directly compared for changes in morphology and integrated flux of various features. In general the 6 cm maps show no significant difference in integrated flux to within the errors (see Table 1). Moreover, a differenced map produced from the two data sets taken at epochs separated by 495 days (1982 September 26–1984 February 3) indicates that the data are quite similar; minor map differences may be explained by less complete parallactic angle coverage and/or the factor of ~ 1.4 more noise on the more recent 6 cm map due to less on-source integration time and fewer available antennas. Moreover, since the 1982 data set was much more extensive than the 1984 data set, we selected only part of the 1982 data in order to approximate more closely the 1984 observations. When these data were processed, qualitative morphological agreement was much more apparent. Thus, we have not been able to detect any significant difference in these two radio data sets apart from stronger persistence of feature A′ in the 1984 data set as compared to the 1982 data set; this was even more dramatic when the subset of the 1982 produced no indication of feature A′. Recently Mauron *et al.* (1984) have confirmed the reality of features A and A′ from near-UV observations. The optical map in Figure 2 shows that the radio morphology of the jet (feature B) has not changed over the past few years and indicates that the optical and radio emitting regions are cospatial.

First attempts to create 2 cm maps of the jet failed because no taper was applied. In order to more closely approximate the 6 cm beam, an 80 kilowavelength taper was applied to the 2 cm data during the cleaning process; this procedure clearly brings out the boundaries of the jet for the first time (see Fig. 1), allowing integrated fluxes to be obtained (see Table 1). We hasten to point out that since the 2 and 6 cm maps herein have approximately the same beam size, spectral indices of features determined from these two maps are less suspect. To detect weaker features at 2 cm like feature A in the 6 cm maps, we estimate that a factor of 4 increase in integration time with the same equipment configuration and correspondingly greater parallactic angle coverage would be required.

The 20 cm map of R Aquarii and the 2, 6, and 20 cm maps of the CDRS were all processed with no taper applied. Figure 1 of R Aquarii at 20 cm shows that the jet and the compact H II region surrounding the hot companion are approximately the same in flux (see Table 1) and that resolution at this wavelength is too low to reveal weak features (e.g., feature A which is readily apparent in the 6 cm map). The CDRS maps are not shown here but will be the subject of a future paper; however, at 6, 20, and 2 cm the stronger component is linearly polarized at $\sim 10\%$, $\sim 4\%$, and $< 2\%$ levels, respectively. Moreover, no CDRS optical emission was detected to a limiting level of $V \approx +20$ (see § II*b*). Additionally, we determine a spectral index of ~ -1.3 for the CDRS. We conclude that the CDRS is an extragalactic background radio object due to its strong linear polarization, highly negative spectral index, and no apparent optical counterpart.

None of the radio features in the R Aquarii maps at 2, 6, or 20 cm reveal any significant degree of linear polarization; all such determinations were less than $\sim 3\%$ and no polarization vectors were obtained above a 3 σ map noise level. Table 1 gives spectral indices for individual features detected in 2, 6, and 20 cm maps of R Aquarii. From Table 1 and the absence of linear polarization of any feature, we conclude that the jet and the compact H II region are both thermal in nature; moreover, the jet's spectral index, $\alpha(\text{jet}) \approx 0$, indicates the optically thin case, while the compact H II region's spectral index, $\alpha(\text{R Aqr}) \approx +0.6$ is the one expected for a spherically symmetric steady mass outflow at constant speed (cf. Wright and Barlow 1975; Panagia and Felli 1975; and Abbott *et al.* 1980 who discuss the radio spectral index for an optically thick expanding wind). Figure 3 shows the spectral graphs with the

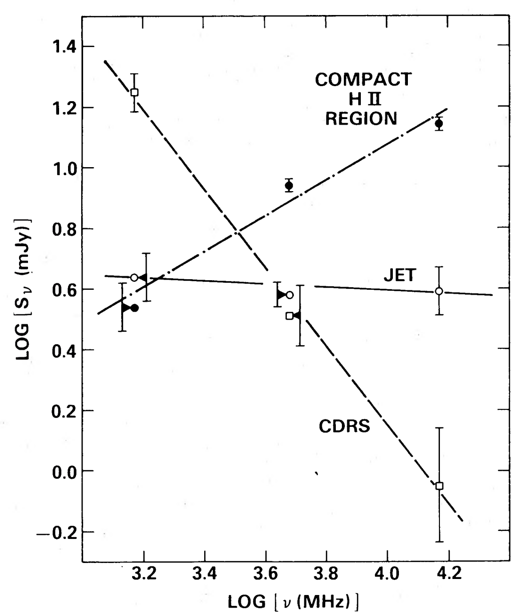

FIG. 3.—Shown are the regression lines which determine the spectral indices of the CDRS, the compact H II region around the hot companion, and the jet $\sim 6''$ northeast of the LPV. Actual values of the spectral indices are presented in Table 1.

regression lines which determine the spectral indices for the jet, the compact H II region, and the CDRS as well.

IV. DISCUSSION

The observed thermal emission from the R Aquarii symbiotic system and its jet can be used to obtain nebular parameters.

The model introduced by Seaquist, Taylor, and Button (1984) and the more detailed work by Taylor and Seaquist (1984), which allows this model to be applied to individual systems, have been applied to the radio emission from R Aquarii; hereafter we will refer to these authors and their related work as STB. In their model, STB propose that a wind from the LPV in a symbiotic system is photoionized by the hot companion. In principle, the STB model can provide values for the LPV wind density, orbital separation, and ionizing flux, although in practice uncertainties involving the viewing angle of the system and the exact frequency at which the free-free optical depth approaches unity make it difficult to obtain all of the above values uniquely. Because $\alpha(\text{R Aqr}) \approx +0.6$ and the binary orbit viewing angle is $\sim 0°$ or seen edge-on (cf. Willson, Garnavich, and Mattei 1981; Kafatos and Michalitsianos 1982), we find the characteristic STB model parameter $X \approx 0.5$ from inspection of the STB theoretical curves. X defines the location of the ionization front and is proportional to $aN_i(\dot{M}/V)^{-2}$, where a is the semi-major axis of the orbit, N_i is the number of ionizing photons emitted by the hot companion, $\dot{M}$ is the mass loss rate from the LPV, and V is the terminal wind velocity. For a distance of 300 pc to R Aquarii (Kafatos, Hollis, and Michalitsianos 1983), our STB model yields $N_i \approx 1.4 \times 10^{44}$ photons s^{-1}, $a \approx 3.2 \times 10^{14}$ cm, and $\dot{M}/V \approx 6.8 \times 10^{-9}$ in units of $(M_\odot \text{ yr}^{-1})/(\text{km s}^{-1})$.

We now compare the R Aquarii STB model just derived to other estimates of N_i, a, and $\dot{M}$ tabulated by other investigators: From *IUE* observations Michalitsianos, Kafatos, and Hobbs (1980) obtained N_i in the range 5×10^{43}–2×10^{44} photons s^{-1}, for effective temperatures of the hot subdwarf in the range 5×10^4–10^5 K, respectively. Agreement between the STB model value for N_i and the *IUE* result is excellent. Also, Kafatos and Michalitsianos (1982), using *IUE* and radio data, obtained $a \approx 2.5 \times 10^{14}$ cm which is consistent with a binary period, P, of 44 years and a combined mass of the two component stars of a few solar masses, assuming that the LPV has a mass of $\sim 1.5\ M_\odot$ (cf. Michalitsianos and Kafatos 1978). Moreover, Michalitsianos, Kafatos, and Hobbs (1980) determined $\dot{M} \approx 10^{-7}\ M_\odot$ yr^{-1}, assuming a constant density for the compact H II region that surrounds R Aquarii. Using this same assumption, our radio results yield $\sim 2.7 \times 10^{-7}\ M_\odot$ yr^{-1} in the case of a spherically symmetric steady mass outflow at a constant speed of $V \approx 50$ km s^{-1} which is appropriate to the escape velocity of a $1.5\ M_\odot$ LPV, with a radius of $\sim 250\ R_\odot$ (Kafatos and Michalitsianos 1982). So it is not surprising that the STB model yields an $\dot{M}$ consistent with all these other determinations, namely $\dot{M} \approx 3.4 \times 10^{-7}\ M_\odot$ yr^{-1}, assuming $V \approx 50$ km s^{-1}; this slightly larger mass loss rate may be attributed to the smaller emitting volume due to LPV shadowing in the STB binary model as compared to completely ionized wind models of single stars.

We have shown that the assumption of a constant density for the compact H II region and a rather simple analysis of both *IUE* and radio data lead to quite similar results, which are also consistent with results found from the more elaborate STB analysis. Our high-resolution VLA observations of R Aquarii indicate that it may be difficult to apply the analysis of STB to more distant symbiotics. If R Aquarii were at a distance ≥ 1000 pc which is more typical of most symbiotics (Michalitsianos *et al.* 1982), it would be difficult to resolve individual structure. In any case, one could not easily separate associated external H II regions from the H II nebular emission surrounding a hot companion as we have done here. Regarding the immediate vicinity of R Aquarii, the spectral index of the combined flux turns out to be $\sim +0.36$ which represents neither $\alpha(\text{jet}) \approx 0.0$ nor $\alpha(\text{R Aqr}) \approx +0.6$ which we have shown to be the case here. As STB acknowledge, their analysis, based solely on the combined spectrum, is susceptible to systematic error when optically thin emission is also present. It should be noted that R Aquarii is an unusual system. Most symbiotics have integrated spectral indices greater than $+0.6$. Flatter spectra (e.g., $+0.36$ in the case of R Aqr) are rare and appear to occur among the dust-type rather than the stellar type infrared emitting symbiotics (see Seaquist, Taylor, and Button 1984).

It follows that a constant density nebula originating from an LPV stellar wind is consistent with both the UV and radio observations, does explain the origin of the compact nebula surrounding R Aquarii, but does *not* explain the sudden appearance of the jet $\sim 6''$ away from R Aquarii some 6 years ago. Our radio observations of the jet can be used to address this problem. For example, since the jet is optically thin and $\sim 3''$ in diameter, we obtain $n_e \approx 7 \times 10^3$ cm^{-3}; this result is weakly dependent on the electron temperature which is assumed to be $\sim 10^4$ K. Moreover, Michalitsianos and Kafatos (1982) obtain $n_e \approx 1.9 \times 10^4$ cm^{-3} using *IUE* data. We conclude that $n_e \approx 10^4$ cm^{-3} is a good estimate for the jet whose total mass would then be $\sim 7 \times 10^{-6}\ M_\odot$ with a kinetic energy limit of $\leq 7 \times 10^{43}$ ergs, assuming $V \leq 1000$ km s^{-1}. A velocity of this order would be required if the jet were formed ~ 6 years ago by episodic transfer of material as proposed by Kafatos and Michalitsianos (1982). There are other arguments favoring this formation mechanism. We note that if the jet were moving with the LPV wind velocity it would have been ejected ~ 185 years ago! Moreover, if the jet were a feature of such a wind, an assumed r^{-2} density law would predict a jet density of only 250 cm^{-3}. Additionally, since we have shown the mass of the jet to be at least $10^{-6}\ M_\odot$, a highly anisotropic LPV mass loss rate of at least $\sim 10^{-6}\ M_\odot$ yr^{-1} would be required for the jet to suddenly appear.

Table 3 summarizes the parameters that characterize the properties of the nebular emission features which comprise the R Aquarii environment. Values shown in Table 3 for the compact H II region surrounding the hot companion are the same as presented in our *IUE* data analysis. We note that feature A (which must have a diameter $\leq 1''$) would have $n_e \geq 2 \times 10^4$ cm^{-3} and a kinetic energy of $\geq 8 \times 10^{42}$ ergs. The jet remains the dominant energetic feature in the immediate vicinity of R Aquarii. We also calculate that the jet should become optically thick at ~ 200 MHz. Radio observations of the jet over the next few years are essential in order to detect morphologic changes in the radio environs. In Figure 1 (*center panel*), the more extended A′ radio contours on the southwest side of the central optically thick compact H II region counter to A suggests greater extension ($\sim 1''$) in 1984 when compared to data obtained in 1982 (Fig. 2). If A′ has changed over a time scale of ~ 1.5 years, at a distance to R Aquarii of 300 pc, the extension of these A′ contours in the direction counter to

TABLE 3

PHYSICAL PARAMETERS OF NEBULAR FEATURES

Parameter (1)	Compact H II Region around the Hot Companion (2)	Feature A (3)	Feature B "The Jet" (4)	Extended ~120″ General Nebulosity (5)
T_e (K)	1.5×10^4 [a]	1×10^4 [b]	1×10^4 [a]	1×10^4 [b]
n_e (cm^{-3})	1×10^6 [c]	$\geq 2 \times 10^4$ [c]	7×10^3 [c]	$\leq 3 \times 10^3$ [c]
Total mass ($M_\odot$)	5×10^{-8} [d]	8×10^{-7} [e]	7×10^{-6}	$\leq 6 \times 10^{-2}$ [f]
Velocity (km s^{-1})	~50[g]	~1000	≤1000	~50–100[h]
K. E. (ergs)	...	$\geq 8 \times 10^{42}$	$\leq 7 \times 10^{43}$	$\leq 6 \times 10^{45}$
Cooling time (yr)	0.02	≤1	3	≥6
Cooling rate (ergs yr^{-1})	1×10^{40}	$\leq 4 \times 10^{39}$	1×10^{40}	$\leq 4 \times 10^{43}$

[a] Michalitsianos and Kafatos 1982.
[b] Typical electron temperatures from Wallerstein and Greenstein 1980.
[c] Present work, assuming a constant density nebula.
[d] Assuming a radius of 2.5×10^{14} cm from Kafatos and Michalitsianos 1982.
[e] Assuming a maximum size of 1″.
[f] Assuming a radius of 40″.
[g] Assuming that this nebula is an optically thick LPV wind; however, one could assume it to be a stationary H II region.
[h] Baade 1944.

feature A suggests velocities ~1000 km s^{-1}. Obviously this suggestion can and should be checked with future VLA observations. The fact that the jet (feature B) appears to be virtually stationary at these two epochs may indicate rapid deceleration following mass ejection from the system. If there were no motion of the jet away from the R Aquarii system over a period of 10 years, it would indicate an upper limit to the terminal velocity of ≤150 km s^{-1}. A comparison of high spatial resolution VLA data obtained a few years apart would be the best way to determine whether the jet and associated features were formed as a result of an episodic mass transfer event in the late 1970s which led to the sudden expulsion of matter (Kafatos and Michalitsianos 1982); or whether such features may be explained as density enhancements in the LPV wind (Spergel, Giuliani, and Knapp 1983).

However, models which interpret the origin of the radio features as the result of condensation of globules in the LPV wind do not adequately explain a number of important features of the optical and radio data: First, the jet (feature B; Fig. 1) contains more mass than the compact H II region surrounding the hot companion by a factor ~200 and is not consistent with a r^{-2} dependence for the density distribution. Second, the jet's size, based on our radio observations, is much greater by a factor of ~30 compared to the entire binary orbit; such a size argues against a condensation due to hydrodynamic instability in the LPV wind as Spergel *et al.* propose. In fact Spergel *et al.* find a characteristic size for the clumps of 2×10^{14} cm which is at odds with the higher spatial resolution (~1″ limiting resolution) 6 cm resolution VLA maps shown here. Third, from optical imagery of the nebula (cf. Sopka *et al.* 1982), we find no evidence of a shadowing effect at distances comparable to the separation of feature B and the R Aquarii compact H II region. Fourth, in our most recent VLA observations, evidence for a radio feature appearing diametrically opposite feature A (Fig. 2–feature A′) is difficult to understand from their model but follows naturally if material is periodically ejected, preferentially along the polar axis of the binary system (Kafatos and Michalitsianos 1982). However, feature B does not have any apparent counterpart observable in the radio; thus, this poses problems for any symmetrical jet model which must invoke special geometries.

V. CONCLUSIONS

With regard to the R Aquarii system, we have unequivocally shown that the compact H II region spectral index is ~ +0.6, indicative of a thermal and optically thick expanding wind from the LPV; that the radio jet emission is optically thin, thermal, cospatial with optical emission, and stable over the last few years; and that the CDRS ~196″ northeast of the LPV emits linearly polarized nonthermal radio radiation with no optical counterpart and, thus, is an extragalactic background object which fortuitously lies along the position angle determined by the LPV and the jet's peak emission. We suggest that features A and A′ may be countermanifestations of symmetric jet action. Moreover, we have shown shortcomings in models which interpret the origin of observed R Aquarii radio features as a result of density enhancements of the LPV wind due to hydrodynamic instabilities; such models (1) fail by a factor of ~200 the assumed r^{-2} density distribution when the density of the jet is compared to that of the compact H II region, (2) propose condensation scale lengths too large by a factor of ~30 as compared to size of the entire binary system, (3) fail to account for no observed optical shadowing effect at distances comparable to the separation of the jet and LPV, and less importantly (4) fail to predict feature–counterfeature morphology suggested by our new observations. Additionally, we have shown that symbiotic stars as a class may be difficult to study since the proximity of R Aquarii has shown it to be quite complex with regard to observed radio features; such features would be unresolved at distances more typical of symbiotic stars, and their aggregate effect may possibly distort the total spectral index to such a degree that application of complicated models could mislead investigators.

We wish to thank Dr. Barry G. Clark for a fine job of arbitrating the proposal review process and Mr. John Wilson for assistance in producing the optical photograph herein. We are grateful to Mr. Dave Van Horn and the VLA staff for obtaining the observations. We appreciate the help of Dr. John R. Dickel, John Simonetti, and Mrs. Peggy Perley during the calibration of the observations. We value the extensive help provided by Dr. R. L. Brown during the map reduction phase as well as his critical comments regarding the final manuscript.

REFERENCES

Abbott, D. C., Bieging, J. H., Churchwell, E., and Cassinelli, J. P. 1980, *Ap. J.*, **238**, 196.
Baade, W. A. 1944, *Rep. Dir. Mt. Wilson Obs.*, **12**.
Baars, J. W. M., Genzel, R., Pauliny-Toth, I. I. K., and Witzel, A. 1977, *Astr. Ap.*, **61**, 99.
Herbig, G. 1980, *IAU Circ.*, 3535.
Kafatos, M., Hollis, J. M., and Michalitsianos, A. G. 1983, *Ap. J. (Letters)*, **267**, L103.
Kafatos, M., and Michalitsianos, A. G. 1982, *Nature*, **298**, 540.
Mauron, N., Nieto, J. L., Picat, J. P., Lelievre, G., and Sol, H. 1984, *Astr. Ap.*, submitted.
McAlister, H. A., Robinson, W. G., and Marcus, S. L. 1982, *Proc. Soc. Photo-Opt. Instr. Eng.*, **331**, 113.
Michalitsianos, A. G., and Kafatos, M. 1978, *Ap. J.*, **226**, 430.
———. 1982, *Ap. J., (Letters)*, **262**, L47.
Michalitsianos, A. G., Kafatos, M., Feibelman, W. A., and Hobbs, R. W. 1982, *Ap. J.*, **253**, 735.
Michalitsianos, A. G., Kafatos, M., and Hobbs, R. W. 1980, *Ap. J.*, **237**, 506.
Panagia, N., and Felli, M. 1975, *Astr. Ap.*, **39**, 1.
Seaquist, E. R., Taylor, A. R., and Button, S. 1984, *Ap. J.*, **284**, 202 (STB).
Sol, H. 1983, *ESO Messenger*, No. 32.
Sopka, R. J., Herbig, G., Kafatos, M., and Michalitsianos, A. G. 1982, *Ap. J. (Letters)*, **258**, L35.
Spergel, D. N., Giuliani, J. L., Jr., and Knapp, G. R. 1983, *Ap. J.*, **275**, 330.
Taylor, A. R., and Seaquist, E. R. 1984, *Ap. J.*, **286**, 263 (STB).
Wallerstein, G., and Greenstein, J. L. 1980, *Pub. A.S.P.*, **92**, 275.
Willson, L. A., Garnavich, P., and Mattei, J. A. 1981, *Inf. Bull. Var. Stars*, Nos. 1961–1963.
Wright, A. E., and Barlow, M. J. 1975, *M.N.R.A.S.*, **170**, 41.

J. M. Hollis and A. G. Michalitsianos: Code 684, Laboratory for Astronomy and Solar Physics, NASA/Goddard Space Flight Center, Greenbelt, MD 20771

M. Kafatos: Department of Physics, George Mason University, Fairfax, VA 22030

H. A. McAlister: Department of Physics and Astronomy, Georgia State University, University Plaza, Atlanta, GA 30303